

A REBAR DETECTION ROBOT

Denis A. Chamberlain

Construction Robotics Unit, Structures Research Centre
City University, Northampton Square
London, EC1V 0HB, England

ABSTRACT

Automation experiments are described which are part of a research programme aimed at the production of an Automated Inspection Facility (AIF) for tall buildings. One of the important tasks for such a facility, the subject of this paper, is rebar detection. The position and orientation sensing requirements of this task, which are similar to those for other inspection tasks, are met using a surface sensing head in conjunction with the rebar locating probe. Using this device, a robot can locate rebars with greater accuracy and speed than a human operator. A suspended vehicle provides good overall access for such a robot in the context of tall buildings.

1. INTRODUCTION

Decay in buildings, particularly in the deterioration of their reinforced concrete fabric, has become a serious and widespread problem. Satisfactory restoration of such buildings relies on correct diagnosis of the underlying causes of decay, which in turn depends on appropriate and reliable inspection methods. In the pursuit of improved reliability, productivity and safety, some commercial successes have been achieved in automating particular inspection tasks^{1,2}. However, whilst research and development programmes are underway^{3,4}, there currently exists no comprehensive sampling and testing facility for tall buildings.

The content of this paper relates to a collaborative research programme aimed at building and evaluating an AIF for tall building inspection⁵. In this, it is intended that a range of inspection tasks will be performed, including rebar detection. This particular test provides information on the approximate location and orientation of rebars, their depth relative to the concrete surface (known as cover) having significant implications for long term durability. Even where reinforcement detail drawings are available, variations between these and the as built component are generally to be expected, particularly in respect to the cover provision.

The operational requirements for automating rebar detection have common points with the automation of other inspection tasks, particularly in the need to maintain position, offset and orientation of the test probe relative to the inspected surface. With this in mind, a general solution has been pursued for setting and maintaining the probe posture. When fully implemented, it is envisaged that the AIF will exchange inspection probes according to the particular test required, plugging these into the surface sensing head.

Following a description of the experimental arrangements, details of the robot, surface sensing head and probe are given. Results of rebar location experiments are also given.

2. AUTOMATION EXPERIMENTS

Two experiments are currently in progress, one in automatic rebar location using a static robot and the other in robot access by means of a suspended support vehicle.

The purpose of the first experiment is to determine the fastest and most reliable search algorithms for known and completely unknown rebar layouts. In the later case, heuristics in the form of object orientated rule sets are employed, these reflecting the probable location and orientation of rebars in relation to findings during patterned searches. Where the approximate layout is known, grid based searches prove to be the most effective.

A light industry SCARA (Selective Compliance Articulated Robot Arm) type robot is used to manipulate a Protovale electro-magnetic rebar locator probe over a specially prepared test piece. Details of this probe and the surface sensing head, which have a combined weight of 1.7kg, can be seen in Figure 1. Figure 2 shows the robot viewed through the test piece, which comprises a 8mm diameter rebar mesh set behind a clear perspex sheet. In this particular test piece, spacing of the mesh decreases from bottom left to top right in regular intervals, the greatest and least spacing being nominally 100mm and 50mm respectively. The gap between the mesh and the perspex sheet can be varied from 30mm to 100mm, thus the effect of rebar depth can be modelled. Positioning the robot for maximum surface coverage, an area measuring 1.0m high by 0.65m wide, is accessed from a single robot location.

The robot operates under closed loop control, using software logic prepared in the C++ language. Analog outputs from its sensors are fed to the controlling microprocessor via an onboard A/D conversion board which samples sensor output at 500 Hz. Both point-to-point and continuous, interpolated path modes can be operated with limits set to accidental contact forces, in order to prevent damage to the robot. Collision avoidance sensing has not been implemented.

Figure 3 shows details of the second experiment in which a Tirfor suspended access vehicle is used to provide overall mobility for the robot. The purpose of this experiment is to study the performance of the robot under such conditions, the dynamic structural interaction between itself and the platform and the effectiveness of damping, bracing and thrust stabilising devices. The deep reinforced concrete beam shown above the robot in Figure 3 is its work piece for rebar detection. A computer controlled counterpart of this vehicle, which is capable of reaching into building recess, is available⁶. In the context of tall buildings, this type of vehicle provides a more general solution to robot mobility than wall climbing devices reported elsewhere^{7,8,9}.

3. SURFACE SENSING HEAD AND REBAR PROBE

The surface sensing head (see again Figure 1) comprises three, highly focused ultra-sonic distance measuring transducers (DMTs) set in a triangular group. Independently, these operate over a 100mm to 800mm range to ± 0.5 mm for target surfaces normals within 10 degrees of the pulse direction. As a near spaced group, they interfere beyond 300mm, but nevertheless perform with their independent accuracy up to that distance, and are thus satisfactory for close sensing requirements. To achieve the full sensing range, the interference condition is automatically detected at the head and two of the sensors cut out. Error in triple sensor detection of inclination to surface is better than ± 0.5 degrees, well within realistic robot performance.

Departure from the operational surface normal condition is detected for single and triple sensing, and is used to trigger target searching. For a single sensor, spherical searches are carried out until the surface is detected and this followed by a refined search for minimum distance where interference is apparent. At close proximity, the single step normality correction set out in the appendix is used with an additional adjustment for offset. This arrangement enables the face of the rebar location probe to be moved in a plane approximately parallel to the surface under inspection. An offset of 2mm-3mm is ideal for this.

The magnetic flux field of the rebar location probe has a distinct orientation, enabling the direction of rebars to be detected by operating the robot's roll axis. For a single rebar, the output passes between maximum and minimum as the flux alignment moves from the aligned to perpendicular orientation with respect to the rebar

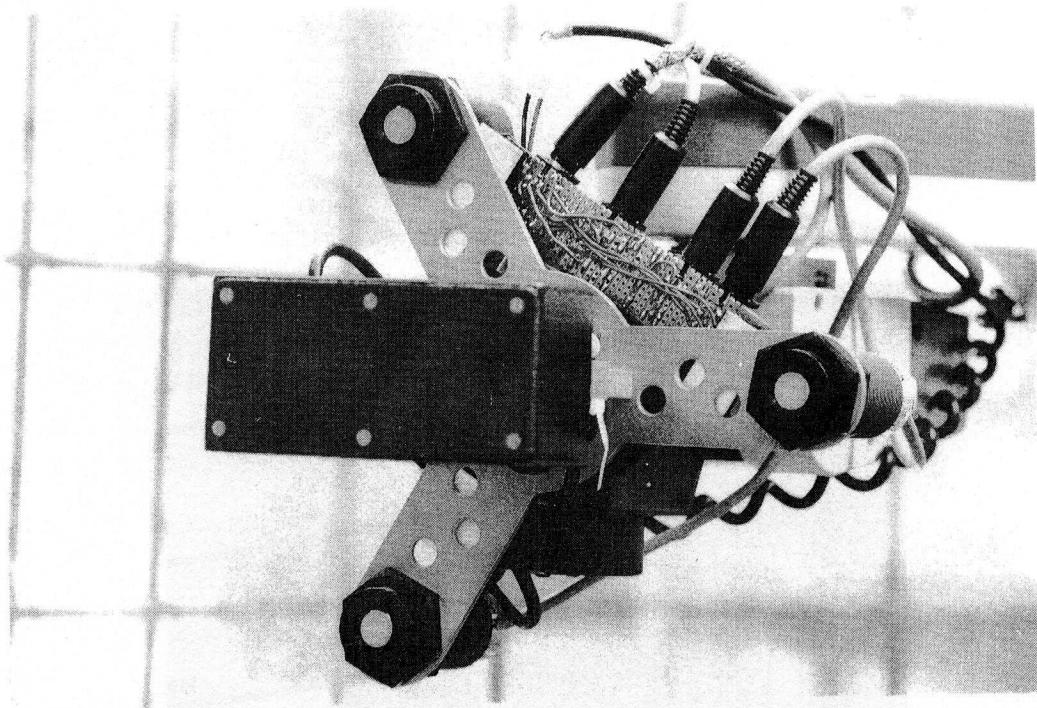


Figure 1. Surface sensor head and rebar probe

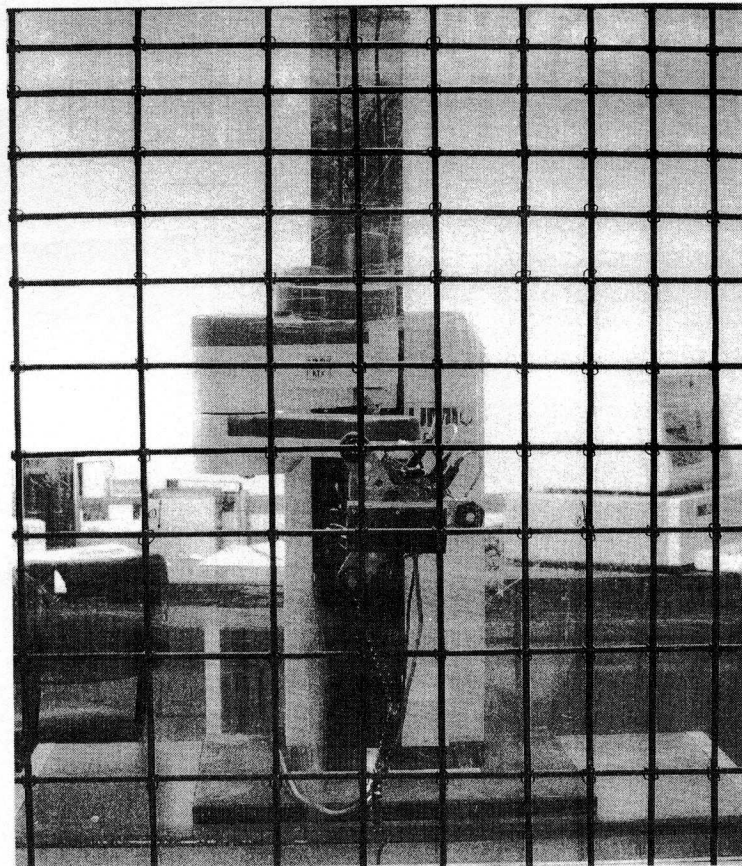


Figure 2. Robot locating rebar mesh

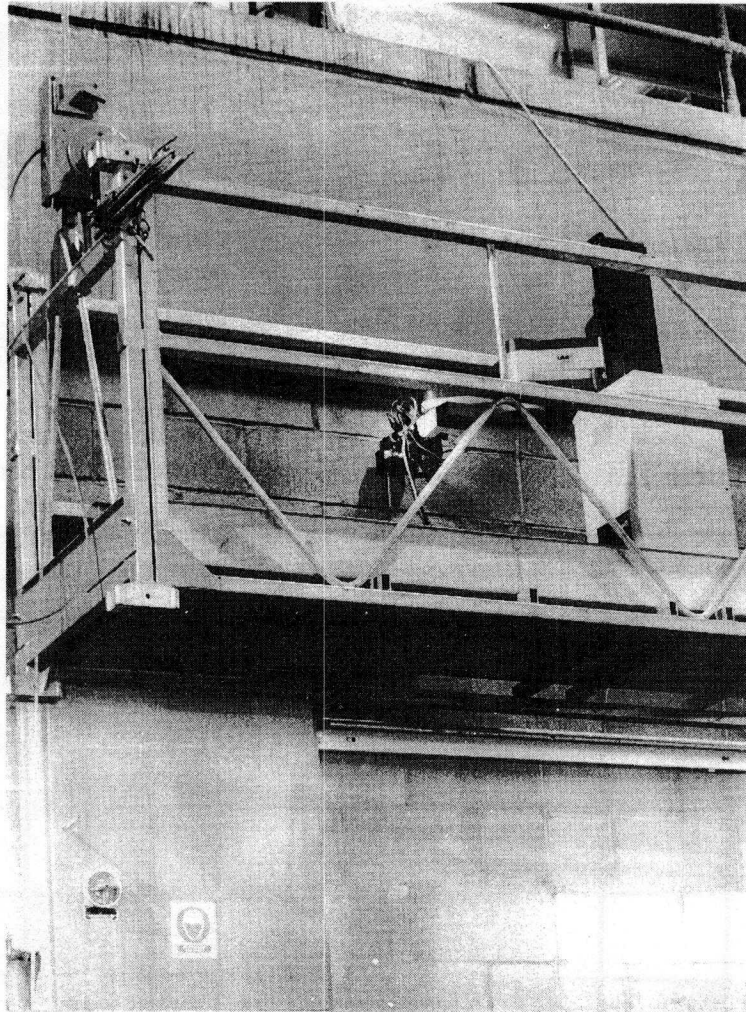


Figure 3. Robot mounted on suspended vehicle

orientation. Once the predominant rebar pattern is established, rebars are quickly located by transverse scans which yield sinusoidal like signal variations. In this, peaks correspond to the theoretical centres of rebars. This is much faster than the manual process, mainly on account of the robot simultaneously providing probe position and value data. The human operator may have to make a number of passes in order to locate a bar, and having done so, he must record its position on the concrete surface for subsequent rebar mapping.

4. EXPERIMENTAL RESULTS.

A typical profile scan and rebar location result is shown in Figure 4. By the automatic process, rebars were located to within $\pm 2\text{mm}$ of their elevational position and to within $\pm 3\text{mm}$ of their cover value up to 50mm cover. Beyond 50mm cover, the cover value error increased linearly to $\pm 7\text{mm}$ at 80mm cover. The robot's worst absolute positioning error under load was found to be within $\pm 2\text{mm}$. The relatively large error in cover value, beyond 50mm cover, appears therefore to be due to rebar location probe rather than the surface sensor head or the robot.

Comparing automatic and manual surveys over the 0.65m² area, the automatic survey was more accurate in respect to rebar positions in the elevation, the manual error being within $\pm 3.5\text{mm}$. No significant differences were found in respect to the accuracy of the cover predictions. However, excluding setting up time, the robot completed the task in approximately 1/3rd of the manual survey completion time. Studies on larger projects with consideration of robot relocation and setting up time are necessary before reliable productivity comparisons can be made.

Initial findings in the access experiment indicate that the robot can perform equally well provided about 0.3kN of horizontal thrust can be delivered to the support structure. Taking the thrust ballast into account, the total weight on the roof level jibs is expected to be 250kg-300kg. However, dynamic loading trials are planned to determine the influence of environmental loadings on the robot's performance.

ONGOING RESEARCH

Investigations are currently in hand to determine the most effective configuration for the AIF. Computer based 3D models of a number of tall buildings have been prepared, these providing a range of access problems including protruding columns, recesses and balconies. Using the GRASP computer simulation facility, various robot configurations are being assessed in terms of their capability and productivity in the execution of set inspection tasks. Figure 5 shows simulated inspection activity on part of a typical tall building.

A man-machine-interface (MMI) for the AIF operator is being developed which includes a high level graphical interface. The facility, which is being prepared using Turbo C++, operates in a multi-tasking window environment. When complete, it will cover requirements for task planning, tele-operations, robot and task monitoring, sensor operations, data handling, faults and alarms. Whilst this has similar facets to others^{10,11}, its particular merit is in the use of 2D and 3D representations of the robot and workpiece which help the operator to understand the AIF's activity and progress. The MMI provision for rebar location is shown in Figure 6. This screen shows the robot configuration, probe scan values, percentage completion and position coordinates. Pull-down menus headers are located at the top of the screen.

6. CONCLUSIONS

Experiments in the use of a robot for automatic rebar location show that good accuracy and productivity can be achieved. However, in the context of building inspection, further investigation is necessary in order to determine the most effective form and configuration of the AIF. Experiments in mounting and operating a robot on a

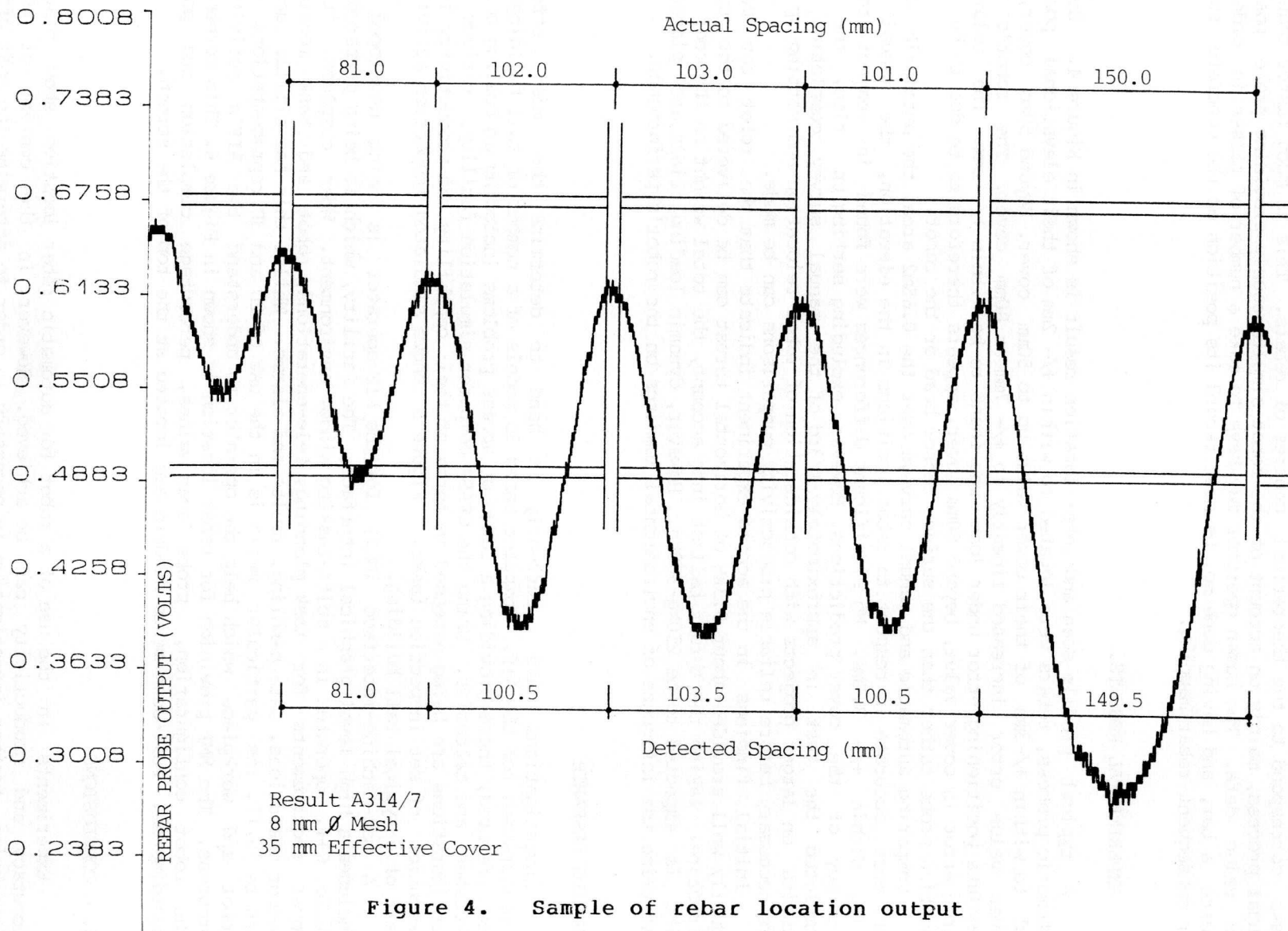


Figure 4. Sample of rebar location output

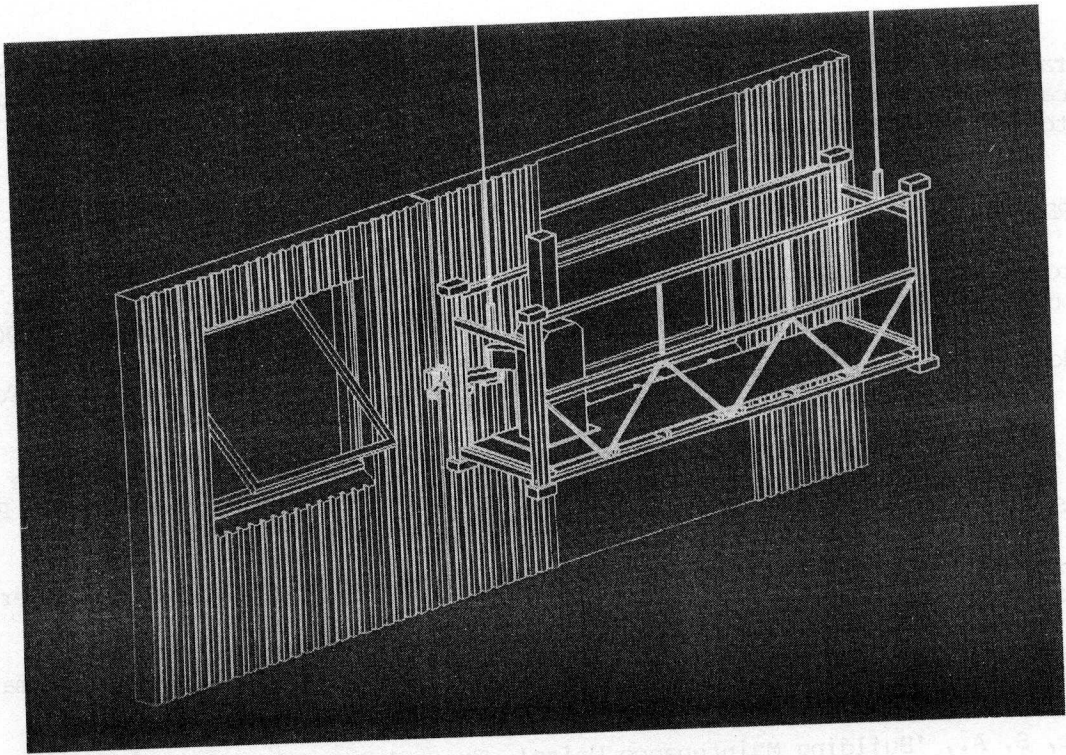


Figure 5. Simulation study on building panel

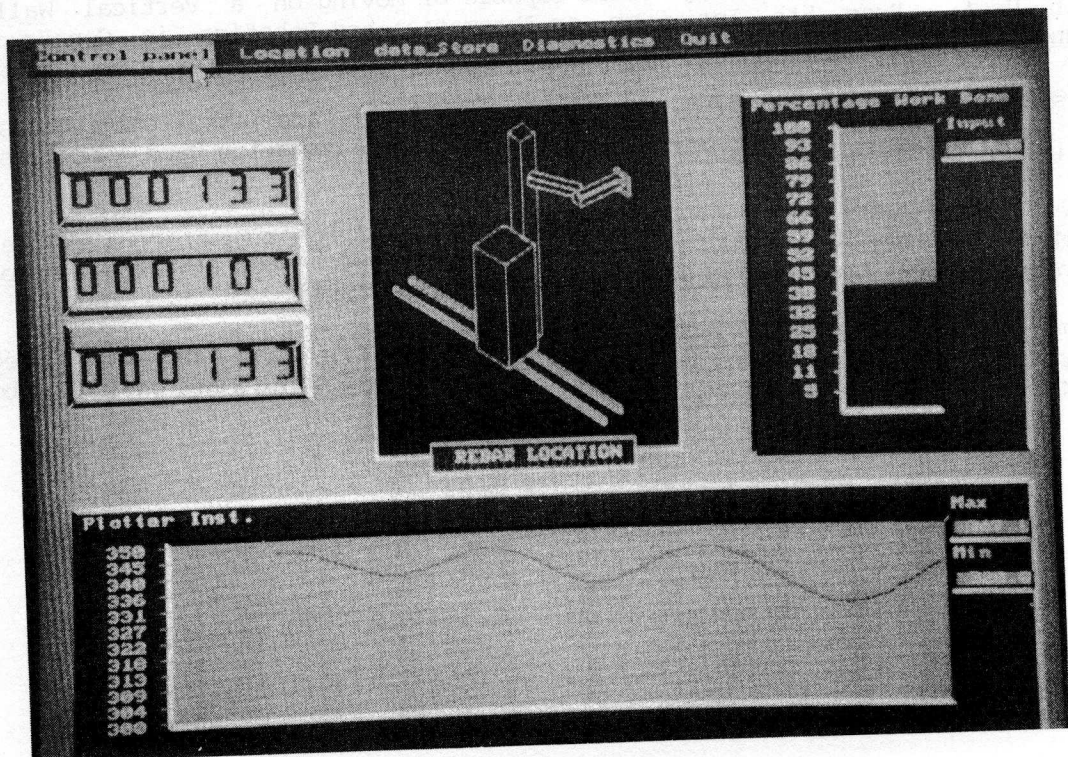


Figure 6. MMI rebar location control screen

suspended access vehicle also show some promise, though further consideration of thrust, bracing and vibration damping is required. The important MMI provision for the rebar locating robot has been presented, this having a graphical interface which aids the operators understanding of the AIF's activity.

7. REFERENCES

1. Hisatomi, Y., 'Introduction of Construction Robotics in Japan', International Association for Bridges and Structural Engineering Journal, J-40/90, February, 1990.
2. Katedoha-Wall, 'Inspection Robot', Ohbayashi Technical Research Institute, Tokyo, 1990.
3. Garas, F. K., 'Development of Advanced Robotics for Inspection, Maintenance and Repair of Buildings and Repair of Buildings and Civil Engineering Structures', Proc. 7th. Int. Symp. on Automation and Robotics in Construction, Bristol, 1990.
4. CEBTP-Lezard, 'Robotics in Construction: Projects and Perspectives', Cahier du CSTB, No. 2412, May 1990, Paris, CSTB, 1990.
5. Chamberlain, D. A., 'A Remotely Operated Building Inspection Cell', Automation in Construction', Pub. Elsevier, Netherlands, April, 1992.
6. Secalt, S. A., 'Building Maintenance Units', Tractel-Group, Luxembourg, 1990.
7. Ikeda, K., Nozaki, T. et al, 'Fundamental Study of a Wall-climbing Robot', Proc. 5th. Int. Symp. on Automation and Robotics in Construction, Tokyo, 1988.
8. Nishi, A., 'Bipedal Walking Robot Capable of Moving on a Vertical Wall for Inspection Use', Proc. 5th. Int. Symp. on Automation and Robotics in Construction, Tokyo, June 1988.
9. Gradetsky, V. and Rachkov, M., 'Wall Climbing Robot and its Applications for Building Construction', Proc. 7th. Int. Symp. on Automation and Robotics in Construction, Bristol, June 1990.
10. White, T. S., Collie, A. A. and Billingsley, C., 'A Robot Climbing Vehicle and its Man-Machine Interface for use in the Nuclear Industry', Proc. 8th. Int. Symp. on Automation and Robotics in Construction, Stuttgart, June 1991.
11. Mikami, T., Hanamori, Y., Ohnishi, T. and Kanno, M., 'An Automatic Direction Control System for Shield Tunneling', Proc. 8th. Int. Symp. on Automation and Robotics in Construction, Stuttgart, June 1991.

APPENDIX

Single step normality correction

Referring to diagrams 1 and 2, a single step normality correction can be achieved using the triple sensing head as follows:

- (i) From the three distance measurements d_1 , d_2 and d_3 , the components of inclination with respect to the local device axes are:

$$A = \tan^{-1} \left[\frac{(d_2 - d_1)}{\ell} \right] \text{ and } B = \tan^{-1} \left[\frac{2d_3 - (d_1 + d_2)}{2m} \right] \quad - \text{Eq (1)}$$

However, the correction for the current roll setting α_r is achieved using the robot's pitch and yaw motors. The required pitch and yaw corrections are thus given by:

$$\Delta\theta_p = \sin^{-1} \left[\frac{\sin C}{\sqrt{1 - D^2}} \right] \text{ and } \Delta\theta_{yw} = \cos^{-1} \left[\frac{\cos C}{\cos \Delta\theta_p} \right] \text{ where } - \text{Eq (2)}$$

$$C = \cos^{-1} \left[-\frac{\cos A \cos B}{\sqrt{1 - \sin^2 A \sin^2 B}} \right], \quad D = \left[\frac{1}{\tan(\alpha_r + E)} \right] \text{ and}$$

$$E = \tan^{-1} \left[\frac{\tan A}{\tan B} \right] \quad - \text{Eq (3)}$$

- (ii) Following these corrections the revised pitch and yaw values:

$$\theta_p = \theta_{ps} + \Delta\theta_p \quad \text{and} \quad \theta_{yw} = \theta_{yws} + \Delta\theta_{yw} \quad - \text{Eq (4)}$$

where θ_{ps} and θ_{yws} are the initial values.

- (iii) An offset correction 'd' can now be performed in the direction defined by:

$$d \left((\cos \theta_p \sin \theta_{yw}) x + (\cos \theta_p \cos \theta_{yw}) y + (\sin \theta_p) z \right) \quad - \text{Eq (5)}$$

The pitch, roll and yaw values are obviously held constant during such moves.

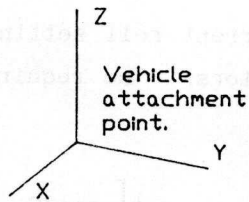
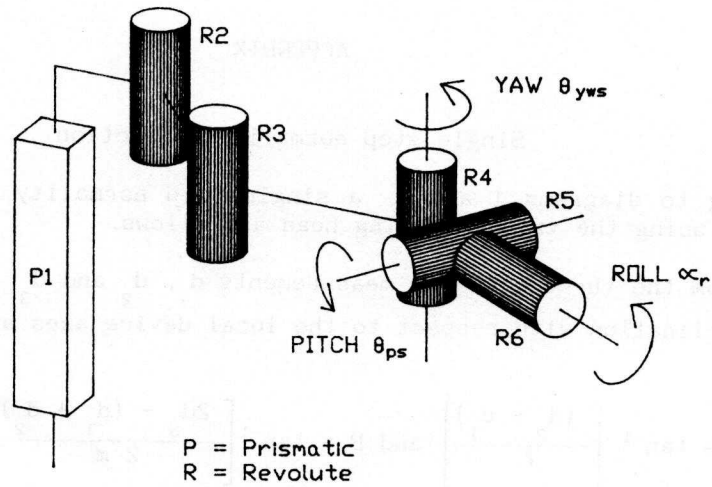


Diagram 1. Robot Configuration Beyond Access Vehicle

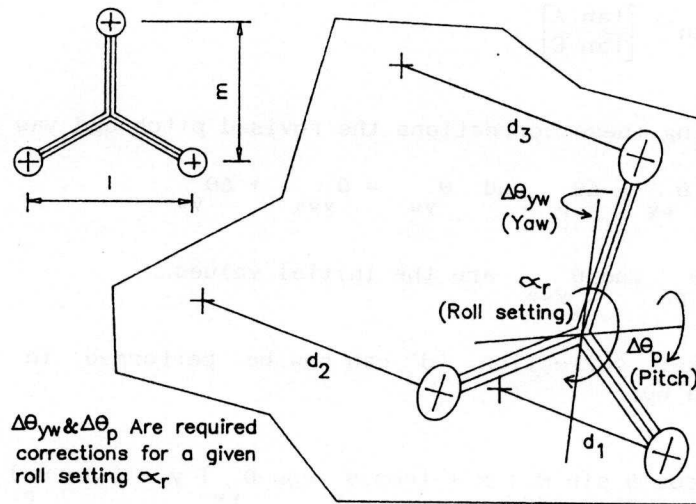


Diagram 2. Sensor Head To Surface Definition